Cancer Management and Research

Dovepress

open access to scientific and medical research

Open Access Full Text Article

ORIGINAL RESEARCH

H19 Rises in Gastric Cancer and Exerts a Tumor-Promoting Function via *miR-138/E2F2* Axis

This article was published in the following Dove Press journal:
Cancer Management and Research

Jingrong Yu[1,*]
Cheng Fang[2,*]
Ziyue Zhang[2]
Guifang Zhang[3]
Lihong Shi[4]
Jiayi Qian[5]
Jianping Xiong[6]

[1]Department of Oncology, The Fourth Affiliated Hospital of Nanchang University, Nanchang, Jiangxi Province 330003, People's Republic of China; [2]Department of Oncology, Nanchang 334 Hospital, Nanchang, Jiangxi Province, People's Republic of China; [3]Department of Obstetrics and Gynecology, The Third Affiliated Hospital of Nanchang University, Nanchang, Jiangxi Province, People's Republic of China; [4]Department of Gynecology and Pediatrics, Nanchang 334 Hospital, Nanchang, Jiangxi Province, People's Republic of China; [5]Department of Ultrasound Electrophysiology, Nanchang 334 Hospital, Nanchang, Jiangxi Province, People's Republic of China; [6]Department of Oncology, The First Affiliated Hospital of Nanchang University, Nanchang, Jiangxi Province 330006, People's Republic of China

*These authors contributed equally to this work

Purpose: The aim of this paper was to investigate *H19* expression in gastric cancer (GC) and its effects on the biological behavior of gastric cancer cells (GCCs), and at exploring its potential mechanism.

Methods: *H19* expression in the patients' tissues and serum was detected, and the correlation of the expression with the patients' pathological data and survival rate was analyzed. Overexpression or inhibitory vectors of *H19*, *microRNA-138* (*miR-138*) and *E2F2* were constructed and transfected into GCCs to observe their effects on the cells' proliferation, invasion and apoptosis.

Results: *H19* rose in GC and was higher in GC patients with a tumor size ≥5 cm, high stages (III+IV) and lymph node metastasis. High H19 expression was associated with the poorer survival rate of the patients, so serum *H19* had a certain diagnostic value for GC. *H19* knockdown could inhibit GCCs to proliferate and invade and induce their apoptosis. *miR-138* can be used as the target gene of *H19*, and *E2F2* can be negatively regulated by this miR, so *miR-138* knockdown or *E2F2* upregulation can weaken GCCs' biological behavior changes that were caused by H19 knockdown.

Conclusion: *H19* can be used as a biological indicator for diagnosing GC and predicting patients' poor prognosis. Additionally, it promotes GCCs to proliferate and invade through *miR-138/E2F2* axis.

Keywords: *H19*, *miR-138*, *E2F2*, gastric cancer

Introduction

As one of the most common cancers and the third leading cause of cancer-related death across the world,[1] gastric cancer (GC) is currently treated based on the combination of surgical operation, radiotherapy and chemotherapy.[2] Although progress has been made in its diagnosis and treatment, patients with the disease still have a poor prognosis due to the high metastasis and recurrence of GC.[3] Therefore, it is urgent to know the potential molecular mechanism of GC development and progression and to find potential therapeutic targets for the disease.

There is more and more evidence that tumor patients experience many kinds of long-chain non-coding RNA (lncRNA) disorders, and that partial disordered lncRNAs are closely correlated with patients' disease progression and prognosis.[4,5] Over 200 nt long, lncRNAs are a series of RNA molecules without protein-coding ability, and they are involved in a variety of biological events via regulating chromatin and transcription as well as gene expression after transcription.[6,7] Having found to be highly expressed in various tumors, *lncRNA H19* (*H19*) is a member of lncRNAs and is considered as a tumor promoter. For

Correspondence: Jianping Xiong
Department of Oncology, The First Affiliated Hospital of Nanchang University, No. 17 Yongwai Street, Nanchang, Jiangxi Province 330006, People's Republic of China
Tel +86-13265847851
Email jpxiong@medmail.com

submit your manuscript | www.dovepress.com
DovePress
http://doi.org/10.2147/CMAR.S267357

© 2020 Yu et al. This work is published and licensed by Dove Medical Press Limited. The full terms of this license are available at https://www.dovepress.com/terms.php and incorporate the Creative Commons Attribution – Non Commercial (unported, v3.0) License (http://creativecommons.org/licenses/by-nc/3.0/). By accessing the work you hereby accept the Terms. Non-commercial uses of the work are permitted without any further permission from Dove Medical Press Limited, provided the work is properly attributed. For permission for commercial use of this work, please see paragraphs 4.2 and 5 of our Terms (https://www.dovepress.com/terms.php).

instance, it plays a carcinogenic role in thyroid cancer through *PI3K/AKT* pathway,[8] and promotes lung cancer cells to proliferate and invade by regulating markers for epithelial-mesenchymal transition.[9] Additionally, it upregulates in GC and predicts the poor prognosis of patients, so downregulating its expression can inhibit gastric cancer cells (GCCs) to invade and migrate.[10] However, the pathway *H19* functions in GC are still unclear.

In this study, the expression and clinical value of *H19* in GC was investigated. Its effects on the biological behavior of GCCs and its potential mechanism were also analyzed. The results may be helpful to further understand the pathogenesis of GC and to find potential therapeutic targets for it.

Materials and Methods

Sources of Clinical Samples

One hundred and twelve GC patients who underwent surgical treatment in the Department of Oncology of the First Affiliated Hospital of Nanchang University from April 2015 to January 2016 were enrolled. Their cancer tissues, normal adjacent tissues and blood were collected during the surgery. Further 112 healthy people undergoing physical examinations during the same period were recruited. Their blood was obtained and stored in a refrigerator (−70°C). Inclusion criteria for patients: Those aged >18 years; those confirmed with GC by pathological examinations; those who signed the informed consent form. Exclusion criteria for patients: Those with other tumors; those who had previously received treatment for cancers; those with incomplete clinical data. This study was approved by the Ethics Committee of the First Affiliated Hospital of Nanchang University and strictly abided by the Declaration of Helsinki.

Cell Sources and Treatment

GCC lines (HGC-27, AGS, MKN-45) and normal gastric mucosal cells (GES-1) were purchased from ATCC cell bank, USA. The cells were placed in a RPMI-1640 medium (Gibco, USA) that contained 10% fetal bovine serum (PBS; Gibco, USA), and the medium was placed in an incubator (37°C, 5% CO_2). Cell transfection: With pcDNA 3.1 plasmids considered as vectors, inhibitory or overexpression plasmids of *H19*, microRNA-138 (*miR-138*) and *E2F2* as well as corresponding negative controls were established. Their transfection was performed using Lipofectamine™ 2000 kits (Invitrogen, USA). Six hours later, the transfected cells were transferred to a 10% PBS-containing medium for culture.

qRT-PCR

qRT-PCR was carried out to detect *H19* and *miR-138* expression, with TRIzol kits (Invitrogen, USA) for total RNA extraction and an ultraviolet spectrophotometer and agarose gel electrophoresis for detecting the purity, concentration and integrity of the RNA. Subsequently, qualified RNA (2 μg) was reversely transcribed into cDNA using reverse transcription kits (TaKaRa, Japan). Next, based on the instruction of SYBR_Premix ExTaq II kits (TaKaRa, Japan), PCR amplification was conducted. The system was 10 μL of SYBR Premix Ex Taq II (2X), 2 μL of cDNA, each 0.8 μL of upstream and downstream primers, and Sterile purified water that was added to supplement to 20 μL. Conditions for the amplification were pre-denaturation (95°C, 30 s), denaturation (95°C, 5 s), and annealing and extension (60°C, 30 s), for a total of 40 cycles. Data analysis was performed using $2^{-\Delta\Delta ct}$.[11] *GAPDH* and *U6* were internal reference genes of *H19* and *miR-138*, respectively. The upstream and downstream primer sequences of *H19* were 5′-TGATGACGGGTGCAGGGGCTA-3′ and 5′-TGATGTTCGCCCTGTCTGCACC-3′. Those of *GAPDH* were 5′-GCACCGTCAAGGCTGAGAAC-3′ and 5′-TGGTGAAGACGCCAGTGGA-3′. Those of *miR-138* were 5′-CGAGAGCTGGTGTTGTGAAT-3′ and 5′-GTGCAGGGTCCGAGGTAT-3′. Those of *U6* were 5′-GTAGCGTCGTGAAGCGTTC-3′ and 5′-GTGCAGGGTCCGAGGTAT-3′.

Western Blotting (WB)

After culture, the cells were cleaved with RIPA lysis buffer (Thermo Fisher Scientific, USA), with BCA protein assay kits (Thermo Fisher Scientific, USA) for protein concentration determination. The loading quantity of sample (40 μg) was taken for 10% polyacrylamide gel electrophoresis (100 V) and PVDF membrane transfer. After sealed in 5% skimmed milk powder for 2 hours, the membrane was cleaned with TBST buffer solution for three times, and then added with *E2F2* (1:1000) and *β-catenin* (1:1000) primary antibodies (Abcam, USA) for sealing all night at 4°C. After washed to remove the antibodies, it was added with goat anti-rabbit IgG antibody (1:1500; Sigma, USA), incubated at 37°C for 1 hour, and finally rinsed with PBS over 5 min for 3 times. After unnecessary liquid was removed, ECL (Millipore, USA) was used for luminescence and

developing. The protein bands were scanned to analyze their gray values in Quantity One. Relative expression levels of the protein = the gray value of target protein band/the gray value of *β-Actin* protein band.

Dual-Luciferase Reporter Gene Assay (DLRGA)

H19-3′UTR wild type (Wt), *H19*-3′UTR mutant (Mut), *E2F2*-3′UTR Wt and *E2F2*-3′UTR Wt were, respectively, established, for respective co-transfection with *miR-138*-mimics or miR-NC into HEK293 cells. Luciferase activities were detected by DLRGA kits (Solarbio, Beijing).

Flow Cytometry for Cell Apoptosis

After digestion with 0.25% trypsin, the cells were added with 100 μL of buffer solution to prepare into a $1*10^6$ cells/mL suspension. Next, the suspension was added with 10 μL of AnnexinV-FITC/PI (Yisheng Biotechnology Co., Ltd., Shanghai) in sequence, for 5-minute incubation at room temperature in dark. A flow cytometry (BD CantoII) was used for analysis, and the apoptotic rate was calculated.

CCK-8 for Cell Proliferation

CCK-8 assay kits (Beyotime Biotechnology, Shanghai, China) were used for detection. Cells were collected after 24-hour transfection, then adjusted to $4*10^6$ cells/well, and finally inoculated on a 96-well plate. After 24-, 48-, 72-, and 96-hour culture, each well was, respectively, added with CCK-8 solution (10 μL) and DMEM (90 μL) for 2-hour culture at 37°C. Next, optical value (OD) values were measured at 490 nm using a microplate reader.

Transwell for Cell Invasion

The cells were adjusted to $1*10^6$ cells/well and inoculated on the upper chamber of the 24-well plate, with 600 μL of the 10% FBS-containing medium added on the lower one. After the Transwell was cultured in an incubator for 24 hours, the matrix and the cells without penetrating the membrane surface in the upper chamber were wiped off. After the cells were cleaned with PBS (3 times), they were fixed with paraformaldehyde (20min), cleaned with double distilled water (3 times), and finally stained with 0.5% crystal violet after they were dried. The cell invasion was observed with a microscope.

Statistical Analysis

In this study, SPSS21.0 (IBM Corp, Armonk, NY, USA) was used to statistically analyze the collected data. GraphPad 7 was used to plot the required figures. The comparison of count data was analyzed by chi-square test or Fisher's exact test, while that of measurement data between two groups was analyzed by independent samples *t* test. One-way analysis of variance (ANOVA) was used for the comparison between multiple groups, followed by Tukey HSD method for verification. Repeated measures ANOVA was used for the comparison between multiple time points, and then Bonferroni was used for test. Kaplan-Meier (K-M) survival curves were plotted to show patients' survival, and Log rank test was used for analysis. A receiver operating characteristic (ROC) curve was plotted to assess the diagnostic value of serum *H19* for GC. When $P<0.05$, the difference was statistically significant.

Results

H19 Expression in GC and Its Clinical Value

According to the qRT-PCR, *H19* upregulated in GC serum, tissues and cells. Based on the analysis of the diagnostic value of serum H19 for GC, its sensitivity, specificity and area under the curve (AUC) were 90.07%, 90.18 and 0.943, respectively. With *H19* expression in patient tissues as the median, the patients were divided into low and high expression groups, to analyze the correlation of *H19* with patients' clinical pathological data and survival rate. High H19 expression was related to a tumor size ≥5 cm, high stages (III +IV), lymph node metastasis and a poor survival rate. This suggests that this RNA is involved in GC pathogenesis and may act as an oncogene. See Table 1 and Figure 1.

H19 Knockdown Can Inhibit GCCs to Proliferate and Invade

In this part, we explored the effects of *H19* knockdown on the biological behavior of MKN-45 and AGS cells (H19 had the largest differential expression in the two cells). According to the CCK-8 assay, cell proliferation was inhibited in the si-*H19* group compared with the si-NC group. According to the Transwell, the number of cells penetrating the membrane reduced in the si-*H19* group compared with the si-NC group. According to the

Table 1 Correlation of *H19* with Clinical Pathological Data

Groups		n	H19		χ^2	P
			Low Expression Group (n=56)	High Expression Group (n=56)		
Gender					2.396	0.122
	Male	68	30 (53.57)	38 (67.86)		
	Female	44	16 (46.43)	28 (432.14)		
Age					2.939	0.087
	<60 years old	49	29 (51.79)	20 (35.71)		
	≥60 years old	63	27 (48.21)	36 (64.29)		
Tumor size					1.820	0.177
	≥5cm	45	19 (33.93)	26 (46.43)		
	<5cm	67	37 (66.07)	30 (53.57)		
TNM staging					6.196	0.013
	Stages I + II	65	39 (69.64)	26 (46.43)		
	Stages III+IV	47	17 (30.34)	30 (53.57)		
Lymph node metastasis					6.053	0.014
	Yes	53	20 (35.71)	33 (58.93)		
	No	59	36 (64.29)	23 (41.07)		
Degree of differentiation					5.486	0.019
	Lowly differentiated	42	27 (48.21)	15 (26.79)		
	Moderately + highly differentiated	74	29 (51.79)	41 (73.21)		

flow cytometry, the apoptotic rate rose in the si-*H19* group compared with the si-NC group. See Figure 2.

H19 Can Negatively Regulate *miR-138*

For understanding the potential mechanism of *H19* in regulating the biological behavior of GCCs, we predicted its potential targeted miRs using starBase3.0 finding that *miR-138* and *H19* have targeted binding sites. For further verifying their relationship, we conducted DLRGA, and found that *miR-138*-mimics could inhibit *H19*-3′UTR Wt luciferase activity, with no remarkable effect on *H19*-3′UTR Mut luciferase activity. In addition, we tested the effects of si-*H19*transfection on *miR-138* in GCCs. This miR rose in the cells after transfection. Subsequently, we explored the effects of miR-138 upregulation on the biological behavior of GCCs. Compared with the miR-NC group, *miR-138* rose, cell proliferation and invasion reduced, and the apoptotic rate rose in the *miR-138*-mimics group. See Figure 3.

miR-138 Can Play an Anti-Cancer Role in GC Through *E2F2*

miRs can affect the basic biological behavior of cells by regulating target genes. For further exploring the mechanism of *H19*/*miR-138* regulating GCCs' biological behavior, we found that *E2F2* and *miR-138* had targeted binding sites through a prediction software for miR target genes. Therefore, we detected *E2F2* changes in cells transfected with miR-NC and *miR-138*-mimics, and found that *E2F2* reduced after *miR-138*-mimics transfection. According to the DLRGA, *miR-138*-mimics could inhibit *E2F2*-3′UTR Wt luciferase activity, with no remarkable effect on *E2F2*-3′UTR Mut luciferase activity. Next, we tested the effects of *E2F2* knockdown on GCCs' proliferation, invasion and apoptosis. Similar to the results of si-*H19* and *miR-138*-mimics transfection, si-*E2F2* transfection could also enhance the proliferation and invasion and reduce the apoptotic rate, and the co-transfection of si-*E2F2* and *miR-138*-inhibitor could reverse the effects of si-*E2F2* on the biological behavior. See Figure 4.

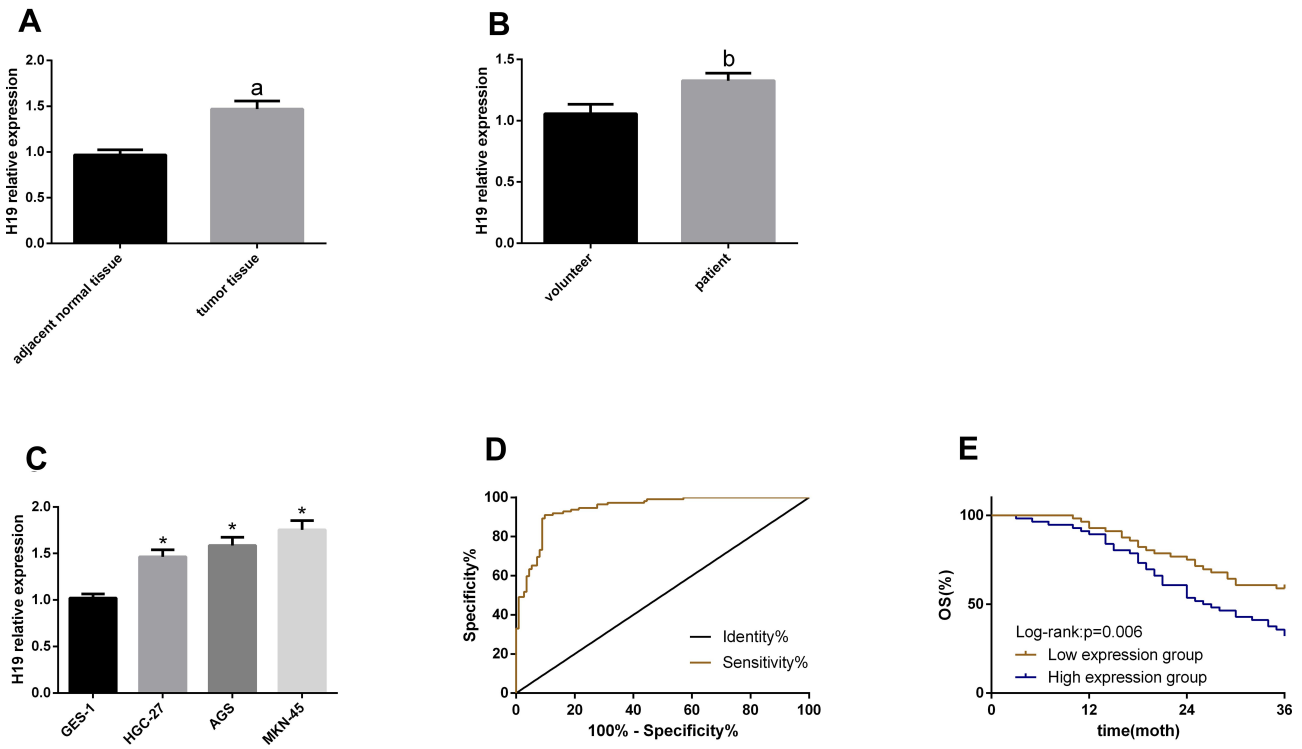

Figure 1 *H19* expression in GC and its clinical value. (**A**–**C**) *H19* upregulated in GC serum, tissues and cells. (**D**) The ROC curve of serum *H19* for diagnosing GC. (**E**) The 3-year overall survival in the high expression group was lower than that in the low expression group.
Notes: [a]Indicates P<0.05 when compared with normal adjacent tissues. [b]Indicates P<0.05 when compared with volunteer. *Indicates P<0.05 when compared with GES-1.

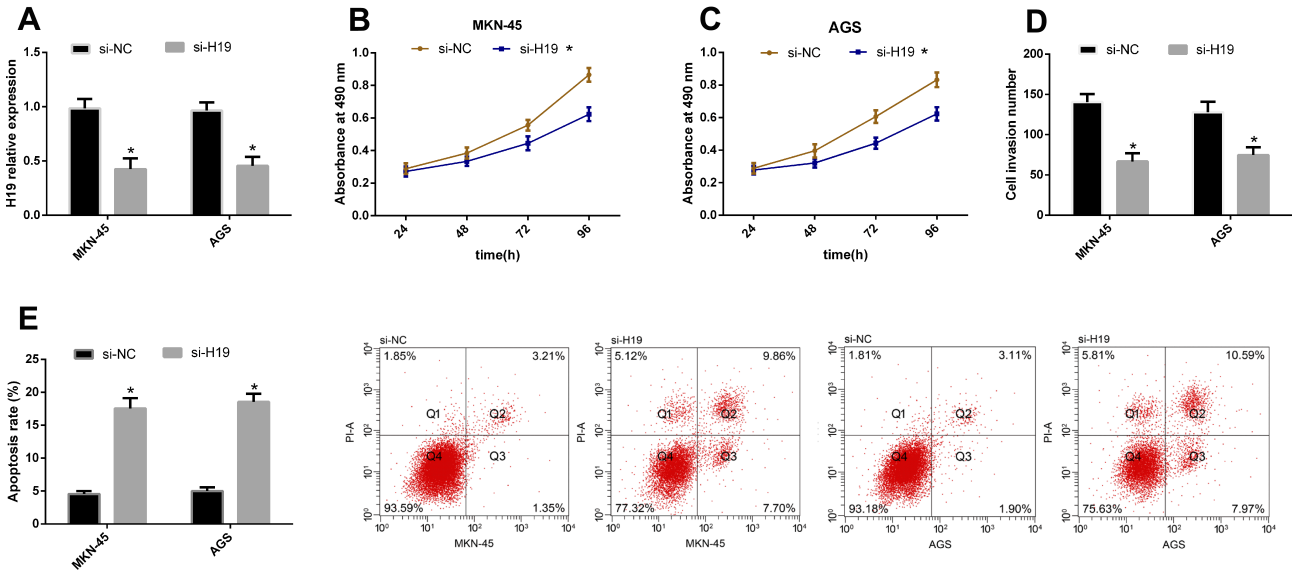

Figure 2 *H19* knockdown can inhibit GCCs to proliferate and invade. (**A**) si-*H19* transfection can inhibit *H19* in GCCs. (**B** and **C**) Cell proliferation reduced after si-*H19* transfection. (**D**) The number of cells penetrating the membrane sharply reduced after si-*H19* transfection. (**E**) The apoptotic rate remarkably rose after si-*H19* transfection.
Note: *Indicates P<0.05 when compared with the si-NC group.

H19 Promotes GCCs' Proliferation and Invasion by Regulating *miR-138/E2F2* Axis

According to the above results, we know that the tumor-promoting effect of *H19* may be related to the *miR-138/E2F2* axis. For further understanding the correlations of the two, we co-transfected GCCs with si-*H19* + *miR-138*-inhibitor and si-*H19* + sh-*E2F2*, respectively, to observe whether such treatment could reverse or weaken the effects of *H19* knockdown

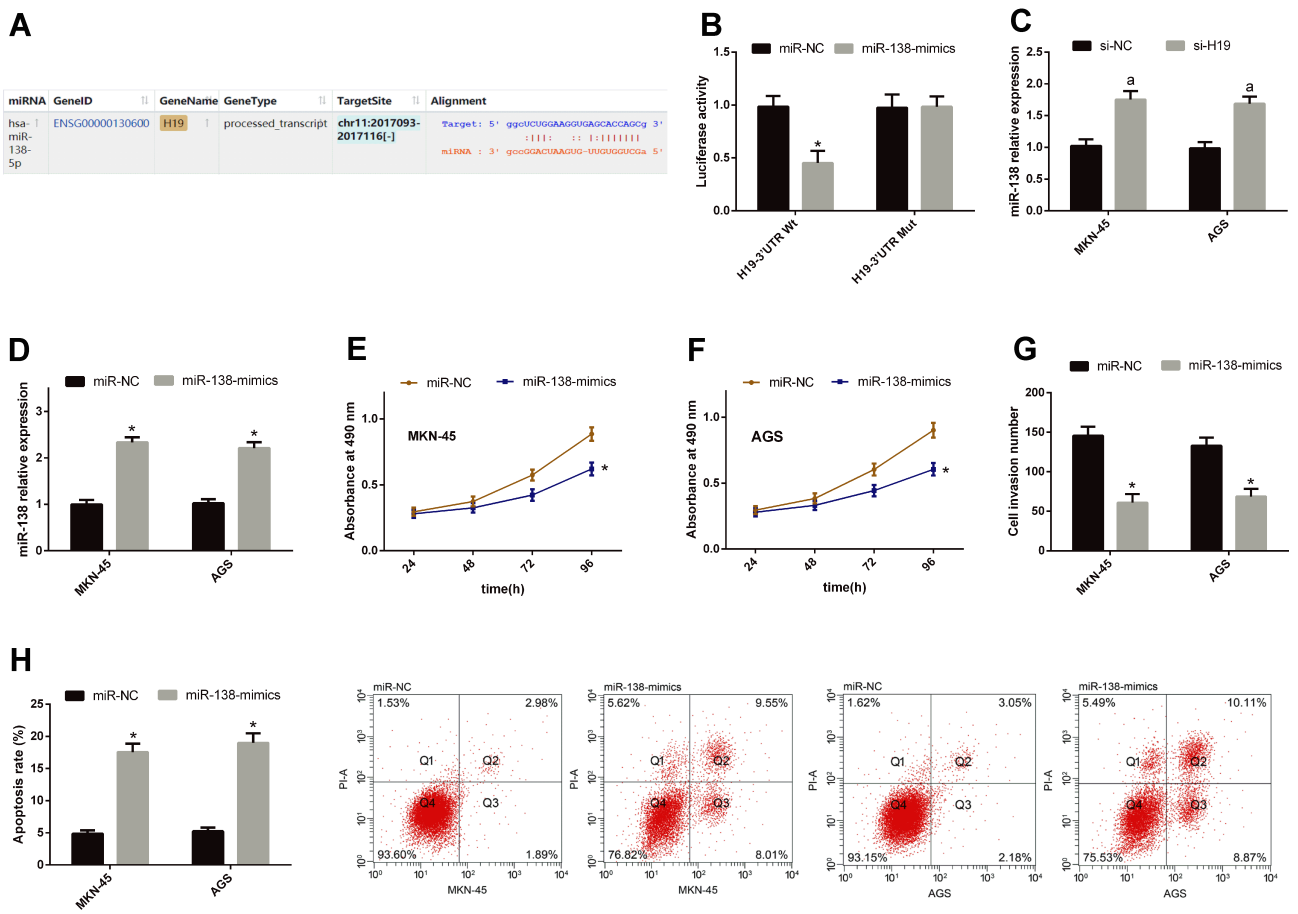

Figure 3 *H19* can negatively regulate *miR-138*. (**A**) *miR-138* and *H19* had targeted binding sites. (**B**) *miR-138*-mimics could inhibit *H19*-3′UTR Wt luciferase activity, with no remarkable effect on *H19*-3′UTR Mut luciferase activity. (**C**) *miR-138* rose in GCCs after si-*H19* transfection. (**D**) *miR-138* rose in GCCs after *miR-138*-mimics transfection. (**E** and **F**) Cell proliferation reduced after *miR-138*-mimics transfection. (**G**) Cells penetrating the membrane were relatively few after *miR-138*-mimics transfection. (**H**) The apoptotic rate rose after *miR-138*-mimics transfection.

Notes: *Indicates P<0.05 when compared with the miR-NC group. [a]Indicates P<0.05 when compared with the si-NC group.

on the cells' biological behavior. The results showed that both co-transfections could reduce changes in cell proliferation, invasion and apoptosis caused by si-*H19* transfection. This shows that *H19* can promote GCCs to proliferate and invade by regulating *miR-138*/*E2F2* axis See Figure 5.

Discussion

At present, targeted therapy in tumor treatment has been recognized by medical personnel, so finding potential therapeutic targets for it is a hot research topic currently. With the continuous understanding of lncRNAs, it has been found that they have a great effect on tumor progression and are considered as potential targets for tumor therapy.[12–14] As one of the earliest lncRNAs found, *H19* (also an oncogene) is located on chromosome 11 and highly expressed in various tumors.[8,9] In our study, we explored the role and mechanism of action of *H19* in GC. *H19* rose in tissues, serum and cells of GC patients, and this increased RNA was related to a tumor size ≥5 cm, high stages (III+IV), lymph node metastasis and a poor survival rate. Based on the analysis of the diagnostic value of serum *H19* for GC, the AUC of *H19* was 0.943. According to the in vivo experiments, *H19* could promote GCCs to proliferate and invade and inhibit their apoptosis. These findings show that *H19* has an extremely high research value, because it is not only a potential biomarker for GC diagnosis and prognosis, but also an important potential therapeutic target for the disease.

More and more studies have revealed that lncRNAs can act as a sponge for miRs, thus regulating levels of target genes downstream of miRs and regulating cell biology.[15] For example, *lncRNA SNGG1* increases *CDK7* expression by competitively binding to *miR-199a-3p*, and then promotes the proliferation and cycle process of prostate cancer cells.[16] *LncRNA CCAT1* may promote retinoblastoma cells to proliferate, migrate and invade, and reduce their apoptosis via the negative regulation of *miR-218-5p*.[17] For exploring the

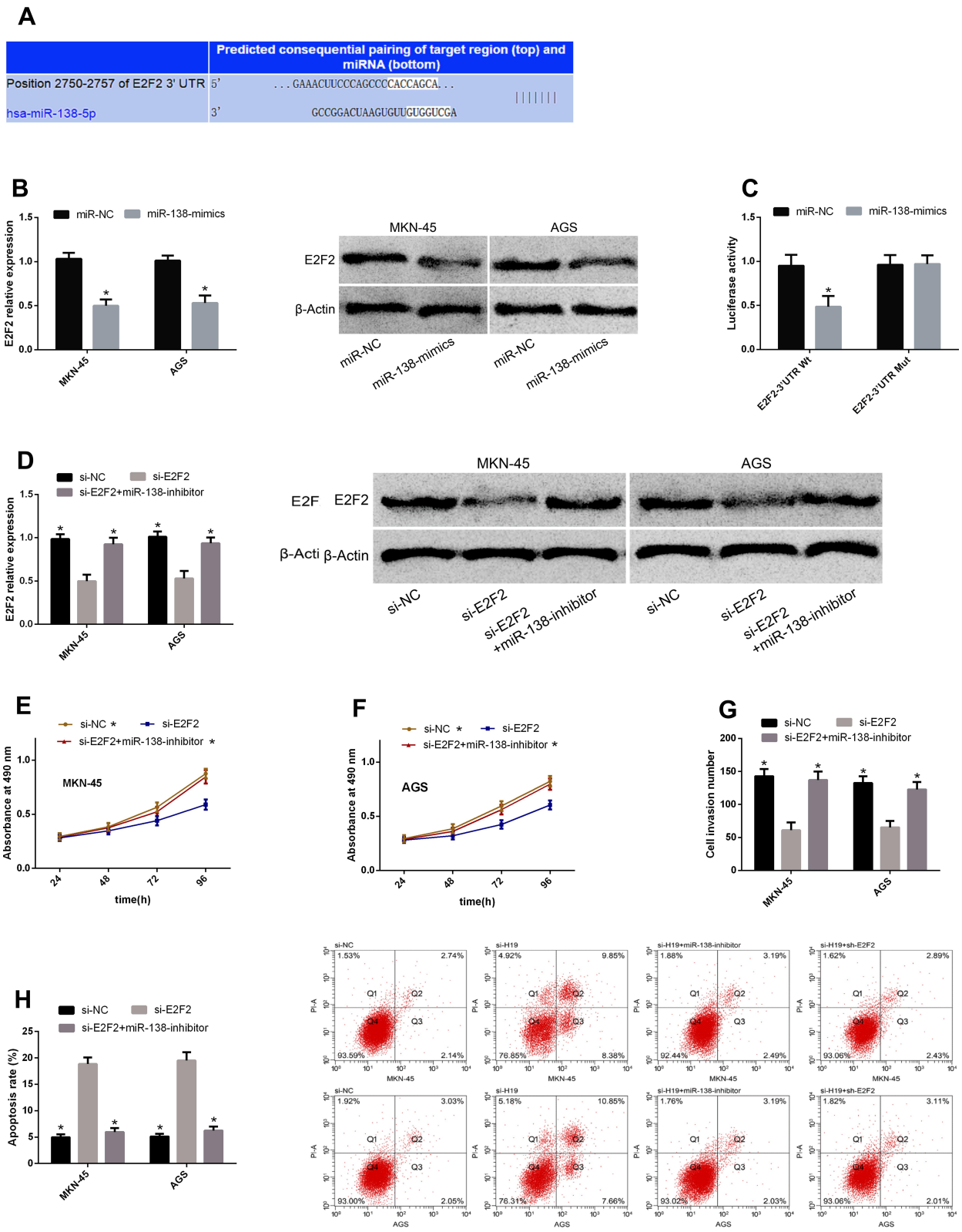

Figure 4 *miR-138* can play an anti-cancer role in GC through *E2F2*. (**A**) *E2F2* and *miR-138* had targeted binding sites. (**B**) *E2F2* reduced after *miR-138*-mimics transfection. (**C**) *miR-138*-mimics could inhibit *E2F2*-3′UTR Wt luciferase activity, with no remarkable effect on E2F2-3′UTR Mut luciferase activity. (**D**) *E2F2* rose after si-*E2F2* transfection, which could be reversed after co-transfection with *miR-138*-inhibitor. (**E** and **F**) Cell proliferation enhanced after si-*E2F2* transfection, which could be reduced after co-transfection with *miR-138*-inhibitor. (**G**) Cell invasion enhanced after si-*E2F2* transfection, which could be reduced after co-transfection with *miR-138*-inhibitor. (**H**) The apoptotic rate rose after si-*E2F2* transfection, which could be reduced after co-transfection with *miR-138*-inhibitor.

Note: *Indicates P<0.05 when compared with the si-E2F2 group.

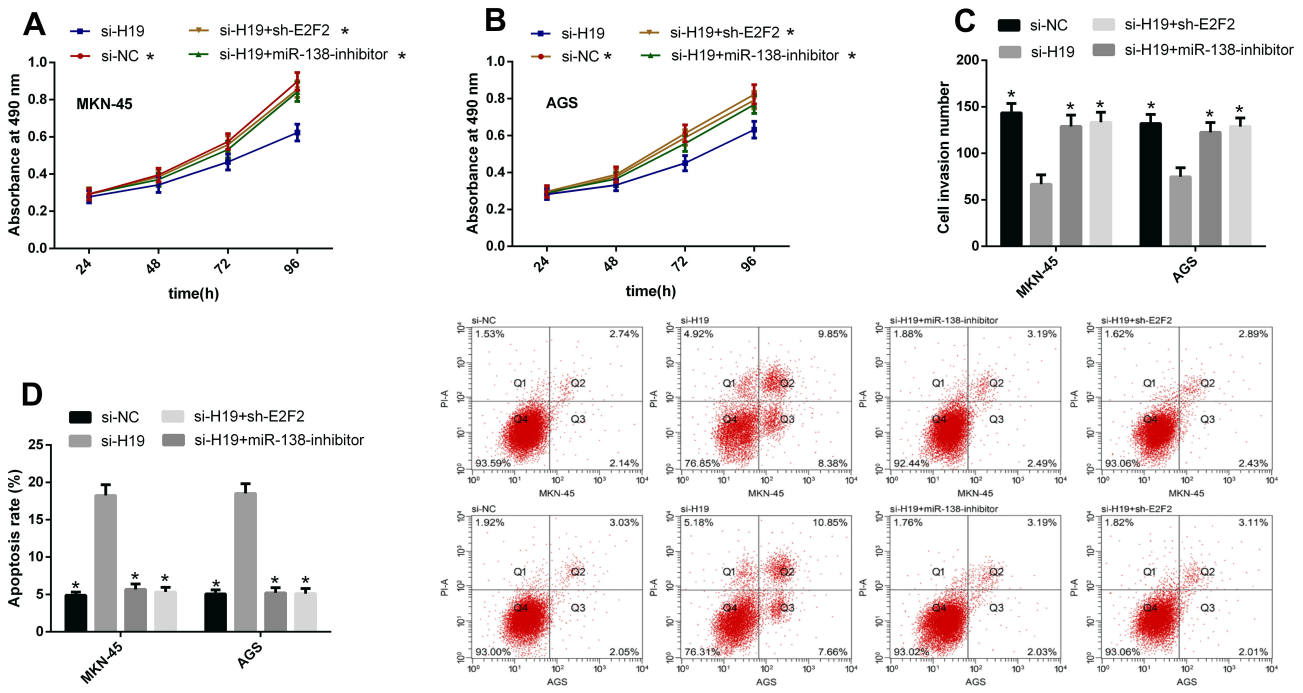

Figure 5 *H19* promotes GCCs' biological behavior by regulating *miR-138*/*E2F2* axis. (**A** and **B**) The co-transfection of both si-*H19* + *miR-138*-inhibitor and si-*H19* + sh-*E2F2* could reduce changes in cell proliferation caused by si-*H19* transfection. (**C**) The co-transfection of both si-*H19* + *miR-138*-inhibitor and si-*H19* + sh-*E2F2* could reduce changes in cell invasion caused by si-*H19* transfection. (**D**) The co-transfection of both si-*H19* + *miR-138*-inhibitor and si-*H19* + sh-*E2F2* could reduce changes in cell apoptosis caused by si-*H19* transfection.

Note: *Indicates P<0.05 when compared with the si-H19 group.

mechanism of action of *H19* in GC and through the biological prediction software starBase3.0, we found targeted binding sites between *miR-138* and *H19*. *miR-138*-mimics could inhibit *H19*-3′UTR Wt luciferase activity, with no remarkable effect on *H19*-3′UTR Mut luciferase activity. *miR-138* rose in GCCs after si-*H19* transfection. These results indicate that there is a certain regulatory effect between *H19* and *miR-138*, so we believe that the effect of *H19* on inhibiting GC progression may be related to this miR. As a kind of highly conservative endogenous short-chain non-coding RNAs, miRs can regulate approximately one third of human genes.[18] Their abnormal expression in human body is considered as an important factor for the development and progression of various diseases.[19–21] Previous studies have found that *miR-138* as a member of miRs downregulates in various tumors including GC.[22–24] In our study, GCCs' proliferation and invasion enhanced but the apoptotic rate rose after *miR-138* upregulation, showing that this miR is a tumor suppressor gene in GC, and that it is expected to become a potential therapeutic target for the disease.

It is well known that miRs are involved in biological processes by regulating downstream target genes. For further improving the mechanism of *H19* and *miR-138* on regulating GCCs' biological behavior, we predicted the downstream target genes of this miR. There were binding sites between *E2F2* and miR-138. E2F2 reduced in GCCs after *miR-138* increased. *miR-138*-mimics could inhibit *E2F2*-3′UTR Wt luciferase activity, with no remarkable effect on E2F2-3′UTR Mut luciferase activity. These results confirm that there is interaction between *E2F2* and *miR-138*. *E2F2* is a member of *E2F2* family, which is an important transcription factor that regulates cell cycle and apoptosis.[25] In tumors, *E2F2* and *H19* are considered as cancer-promoting factors.[26,27] In this article, after *E2F2* knockdown, GCCs' proliferation and invasion reduced but the apoptotic rate rose, and the co-transfection of si-*E2F2* and *miR-138*-inhibitor could reverse effects of the knockdown on the biological behavior. This suggests that *miR-138* and *E2F2* exert a great function in GC progression, and that the two have a mutual regulatory effect. For confirming that *H19* can promote GCCs to proliferate and invade through the miR-138/*E2F2* axis, we knocked down *miR-138* and upregulated *E2F2* while transfecting si-*H19*. The results showed that after such treatment, the effects of si-*H19* on the biological behavior were reversed.

Accordingly, *H19* rises in GC and predicts the poor prognosis of patients, so *H19* knockdown inhibits GCCs to proliferate and invade and induces their apoptosis, which is related to

the *miR-138*/*E2F2* axis. This study has certain limitations. Firstly, due to the short time of this study, more research samples cannot be collected and longer follow-ups cannot be conducted, which results in possibly limited clinical data. Secondly, other mechanisms of H19 are still unclear. We have only studied the *miR-138*/*E2F2* axis, so whether *H19* can promote GC progression through other pathways needs further research.

In summary, *H19* that rises in GC can be used as a biological indicator for diagnosing the disease and predicting patients' poor prognosis, because it promotes GCCs to proliferate and invade through *miR-138*/*E2F2* axis.

Conclusion

In summary, *H19* that rises in GC can be used as a biological indicator for diagnosing the disease and predicting patients' poor prognosis, because it promotes GCCs to proliferate and invade through *miR-138*/*E2F2* axis.

Funding

The authors received no funding for this work.

Disclosure

The authors report no conflicts of interest in this work.

References

1. Bray F, Ferlay J, Soerjomataram I, et al. Global cancer statistics 2018: GLOBOCAN estimates of incidence and mortality worldwide for 36 cancers in 185 countries. *CA Cancer J Clin*. 2018;68(6):394–424. doi:10.3322/caac.21492
2. Wang D, Liu K, Chen E. LINC00511 promotes proliferation and invasion by sponging miR-515-5p in gastric cancer. *Cell Mol Biol Lett*. 2020;25(1):4. doi:10.1186/s11658-020-0201-x
3. Wei J, Xu H, Wei W, et al. circHIPK3 promotes cell proliferation and migration of gastric cancer by sponging miR-107 and regulating BDNF expression. *Onco Targets Ther*. 2020;13:1613. doi:10.2147/OTT.S226300
4. Cui Y, Fan Y, Zhao G, et al. Novel lncRNA PSMG3-AS1 functions as a miR-143-3p sponge to increase the proliferation and migration of breast cancer cells. *Oncol Rep*. 2020;43(1):229–239. doi:10.3892/or.2019.7390
5. Wang B-G, Lv Z, Ding H-X, et al. The association of lncRNA-HULC polymorphisms with hepatocellular cancer risk and prognosis. *Gene*. 2018;670:148–154. doi:10.1016/j.gene.2018.05.096
6. Schmitt AM, Chang HY. Long noncoding RNAs in cancer pathways. *Cancer Cell*. 2016;29(4):452–463. doi:10.1016/j.ccell.2016.03.010
7. Bian Z, Jin L, Zhang J, et al. LncRNA—UCA1 enhances cell proliferation and 5-fluorouracil resistance in colorectal cancer by inhibiting miR-204-5p. *Sci Rep*. 2016;6:23892. doi:10.1038/srep23892
8. Li X, Li Q, Jin X, et al. Long non-coding RNA H19 knockdown inhibits the cell viability and promotes apoptosis of thyroid cancer cells through regulating the PI3K/AKT pathway. *Exp Ther Med*. 2019;18(3):1863–1869. doi:10.3892/etm.2019.7720
9. Liao S, Yu C, Liu H, et al. Long non-coding RNA H19 promotes the proliferation and invasion of lung cancer cells and regulates the expression of E-cadherin, N-cadherin, and vimentin. *Onco Targets Ther*. 2019;12:4099. doi:10.2147/OTT.S185156
10. Chen JS, Wang YF, Zhang XQ, et al. H19 serves as a diagnostic biomarker and up-regulation of H19 expression contributes to poor prognosis in patients with gastric cancer. *Neoplasma*. 2016;63(2):223–230. doi:10.4149/207_150821N454
11. Livak KJ, Schmittgen TD. Analysis of relative gene expression data using real-time quantitative PCR and the 2-ΔΔCT method. *Methods*. 2001;25(4):402–408. doi:10.1006/meth.2001.1262
12. Sun Z, Wu XY, Wu CL. The association between LncRNA HOTAIR and cancer lymph node metastasis and distant metastasis: a meta-analysis. *Neoplasma*. 2018;65(2):178–184. doi:10.4149/neo_2018_170114N34
13. Cao Y, Luo X, Ding X, et al. LncRNA ATB promotes proliferation and metastasis in A549 cells by down-regulation of microRNA-494. *J Cell Biochem*. 2018;119(8):6935–6942. doi:10.1002/jcb.26894
14. Liu Z, Dai J, Shen H. Systematic analysis reveals long noncoding RNAs regulating neighboring transcription factors in human cancers. *Biochim Biophys Acta Mol Basis Dis*. 2018;1864(9):2785–92.
15. Wieczorek E, Reszka E. mRNA, microRNA and lncRNA as novel bladder tumor markers. *Clin Chim Acta*. 2018;477:141–153. doi:10.1016/j.cca.2017.12.009
16. Li J, Zhang Z, Xiong L, et al. SNHG1 lncRNA negatively regulates miR-199a-3p to enhance CDK7 expression and promote cell proliferation in prostate cancer. *Biochem Biophys Res Commun*. 2017;487(1):146–152. doi:10.1016/j.bbrc.2017.03.169
17. Zhang H, Zhong J, Bian Z, et al. Long non-coding RNA CCAT1 promotes human retinoblastoma SO-RB50 and Y79 cells through negative regulation of miR-218-5p. *Biomed Pharmacother*. 2017;87:683–691. doi:10.1016/j.biopha.2017.01.004
18. Li Q, Liang X, Wang Y, et al. miR-139-5p inhibits the epithelial-mesenchymal transition and enhances the chemotherapeutic sensitivity of colorectal cancer cells by downregulating BCL2. *Sci Rep*. 2016;6:27157. doi:10.1038/srep27157
19. Lei C, Du F, Sun L, et al. miR-143 and miR-145 inhibit gastric cancer cell migration and metastasis by suppressing MYO6. *Cell Death Dis*. 2017;8(10):e3101. doi:10.1038/cddis.2017.493
20. Pheiffer C, Dias S, Rheeder P, et al. Decreased expression of circulating miR-20a-5p in South African women with gestational diabetes mellitus. *Mol Diagn Ther*. 2018;22(3):345–352. doi:10.1007/s40291-018-0325-0
21. Li SD, Yang J M, Xia Y, et al. Long noncoding RNA NEAT1 promotes proliferation and invasion via targeting miR-181a-5p in non-small cell lung cancer. *Oncol Res*. 2018.
22. Pang L, Li B, Zheng B, et al. miR-138 inhibits gastric cancer growth by suppressing SOX4. *Oncol Rep*. 2017;38(2):1295–1302. doi:10.3892/or.2017.5745
23. Ye Z, Fang B, Pan J, et al. miR-138 suppresses the proliferation, metastasis and autophagy of non-small cell lung cancer by targeting Sirt1. *Oncol Rep*. 2017;37(6):3244–3252. doi:10.3892/or.2017.5619
24. Wang W, Zhao L-J, Tan Y-X, Ren H, Qi,Z-T. MiR-138 induces cell cycle arrest by targeting cyclin D3 in hepatocellular carcinoma. *Carcinogenesis*. 2012;33(5):1113–1120. doi:10.1093/carcin/bgs113
25. Indovina P, Pentimalli F, Casini N, et al. RB1 dual role in proliferation and apoptosis: cell fate control and implications for cancer therapy. *Oncotarget*. 2015;6(20):17873–17890. doi:10.18632/oncotarget.4286
26. Chen L, Yu JH, Lu ZH, et al. E2F2 induction in related to cell proliferation and poor prognosis in non-small cell lung carcinoma. *Int J Clin Exp Pathol*. 2015;8(9):10545–10554.
27. Feliciano A, Garcia-Mayea Y, Jubierre L, et al. miR-99a reveals two novel oncogenic proteins E2F2 and EMR2 and represses stemness in lung cancer. *Cell Death Dis*. 2017;8(10):e3141. doi:10.1038/cddis.2017.544

Cancer Management and Research

Dovepress

Publish your work in this journal

Cancer Management and Research is an international, peer-reviewed open access journal focusing on cancer research and the optimal use of preventative and integrated treatment interventions to achieve improved outcomes, enhanced survival and quality of life for the cancer patient.

The manuscript management system is completely online and includes a very quick and fair peer-review system, which is all easy to use. Visit http://www.dovepress.com/testimonials.php to read real quotes from published authors.

Submit your manuscript here: https://www.dovepress.com/cancer-management-and-research-journal